Parental assigned chromosomes for cultivated cacao provides insights into genetic architecture underlying responses to *Ceratobasidium theobromae*

Authors: Peri A. Tobias[1]*, Jacob Downs[1], Peter Epaina[1,5], Gurpreet Singh[1], Robert F. Park[1], Richard J. Edwards[2], Eirene Brugman[3], Andi Zulkifli[6], Junaid Muhammad[3], Agus Purwantara[4], David I. Guest[1]

*Author for correspondence: peri.tobias@sydney.edu.au

Affiliations: [1]School of Life and Environmental Sciences, The University of Sydney, Camperdown, NSW, Australia, [2]The University of Western Australia, Perth, WA, Australia [3]Cocoa Research Center Faculty of Agriculture, Universitas Hasanuddin, Makassar, Indonesia, [4]Mars Cocoa Research Station, Pangkep, Indonesia, [5]Cocoa Board of Papua New Guinea, Kokopo, East New Britain Province, Papua New Guinea, [6]Megarezky University, Makassar, Indonesia

Keywords: *Theobroma cacao,* chromosome-level, vascular streak dieback, VSD*,* resistance genes, NLR

Abstract

Diseases of *Theobroma cacao* disrupt cocoa bean supply and have economic impacts to growers. Vascular streak dieback (VSD), caused by *Ceratobasidium theobromae,* is a new encounter disease of cacao currently contained to southeast Asia and Melanesia. Resistance to VSD has been tested with large progeny trials in Sulawesi and Papua New Guinea with the identification of informative quantitative trait loci (QTL). Using a VSD susceptible progeny tree (clone 26), derived from a resistant and susceptible parental cross, we assembled the genome to chromosome-level and discriminated alleles inherited from either resistant or susceptible parents. The parentally phased genomes were annotated for all predicted genes and then specifically for resistance genes of the *nucleotide binding site leucine rich repeat* class (NLR).

On investigation, we determined the presence of NLR clusters at informative QTLs, as well as other potential disease response gene candidates. Understanding the genetics underlying resistance and susceptibility to VSD is likely to accelerate the breeding cycle by providing clear targets for molecular screening. Additionally, we provide the first diploid, fully scaffolded and parentally phased genome resource for *Theobroma cacao* L.

Introduction

Cacao, *Theobroma cacao* L. (Malvaceae) is an important perennial tree crop producing beans that are used as raw materials in the chocolate, beverage, and cosmetic industries (Schnell et al., 2007). Much of the world's cocoa bean production comes from small-holder, mixed cropping farms in some fifty countries that depend on trade with developed countries where the raw product is manufactured into chocolate (Daymond et al., 2022). Cacao is a difficult crop to grow profitably due to several endemic problems. Alongside other problems, diseases disrupt the supply of cocoa and have serious economic impacts to growers (Marelli et al., 2019). Responses to diseased tree losses can lead to removal of trees for more profitable and reliable crops (Daymond et al., 2022). The centre of origin for *T. cacao* is the Upper Amazon rainforest, South America, where evolutionary studies indicate divergence from close common ancestors around 9.9 million years ago (Richardson et al., 2015). While genetic diversity exists within the geographic centre of origin, cultivation largely relies on a limited genetic pool of *T. cacao* (Motamayor et al., 2008). Southeast (SE) Asia is one of the major suppliers of cocoa beans and cultivation and had historically been relatively disease-free due to the lack of co-evolved pathogens (Bailey and Meinhardt, 2016).

Vascular streak dieback (VSD) is a new encounter disease of cacao that first caused devastating crop losses in Papua New Guinea (PNG) in the 1960s (Guest and Keane, 2007). The causal agent *Ceratobasidium theobromae* is a fastidious biotrophic fungus that was first discovered and described by Philip Keane (1972). *Ceratobasidium theobromae* then spread to other SE Asian and Melanesian cacao regions as an emergent disease on cacao (Guest and Keane, 2007). In Indonesia, the pathogen has spread into Sumatera Regions (Trisno et al., 2016) and was subsequently confirmed in a new area of Barru District (Junaid et al., 2020). The pathogen is currently contained to the SE Asia region but presents a serious biosecurity threat to cacao in West Africa and Latin America. Symptoms include green spotted chlorosis in older leaves and vascular browning in the petioles and stems that often leading to rapid

61 branch or whole tree death in susceptible genotypes (Guest and Keane, 2007). Some
62 genotypes of *T. cacao* that were resistant to disease 50 years ago remain resistant, indicating
63 that durable resistance is highly heritable and therefore may be exploited in breeding to
64 introgress resistance into new, improved cacao genotypes.
65 Varieties of cacao that show resilience to infection by *C. theobromae* have been studied in
66 both PNG and Sulawesi, Indonesia. Results of these studies identified informative quantitative
67 trait loci (QTL) that correlate with both qualitative and quantitative resistance in progeny
68 populations (Epaina, 2012; Singh, 2021). The two independent studies used progenies derived
69 from crosses between Trinitario **KA2-101** (resistant to VSD) and **K82** (susceptible to VSD) in
70 PNG (Epaina, 2012), and between Amelonado **S1** (resistant to VSD) with Iquitos, Criollo and
71 Amelonado **RUQ1347** (susceptible to VSD and formerly known as CCN51) in Sulawesi,
72 Indonesia (Singh, 2021). The progeny trials used 346 and 130 progeny that segregated in
73 response to VSD in PNG and Sulawesi, respectively. The informative QTLs associated with
74 resistance indicated a likely polygenic response and were mapped onto nine of the 10 *T. cacao*
75 chromosomes from the PNG progeny trial (Epaina, 2012) and three in the Sulawesi trial (Singh,
76 2021). The two studies used either simple sequence repeat (SSR) or single nucleotide
77 polymorphism (SNP) markers and compared linkage maps with established disease resistance
78 mapping developed by Lanaud et al. (2009). The available genomes for Matina 1-6
79 (Motamayor et al., 2013) and Criollo (Argout et al., 2011) were used to inform the linkage
80 maps. Interestingly, VSD QTLs co-localized with a region identified for resistance to
81 Phytophthora Pod Rot (PPR) and Frosty Pod Rot (FP) (causal agents *Phytophthora palmivora*
82 and *Moniliophthora roreri*, respectively) on chromosome 8, while others were common for
83 response to both VSD and PPR on chromosomes 3, 4 and 5 in only one study. Both studies
84 identified VSD QTLs within similar regions on chromosomes 3, 8 and 9. These apparent shared
85 QTL regions indicate hotspots for disease resistance.
86 Classical selection and breeding for resistance, particularly in perennial trees, can be a long
87 and difficult process (Sniezko, 2006). The research is further complicated for resistance to *C.*
88 *theobromae* as the pathogen cannot be cultured in vitro and is extremely slow growing within
89 the host plant before visible symptoms develop. Traditional Koch's postulates cannot be
90 satisfied for biotrophic organisms, however molecular approaches are becoming increasingly
91 important in validation studies (Bhunjun et al., 2021). Understanding the genetics underlying

92 resistance and susceptibility to VSD is likely to accelerate the breeding cycle by providing clear
93 targets for molecular screening.
94 Effective plant responses to disease at the molecular level are well established as involving
95 resistance genes of the nucleotide-binding site leucine-rich repeat family (NLRs) (Fluhr et al.,
96 2001). NLR genes are known to be numerous, clustered, and highly polymorphic both
97 between and within species (Barragan and Weigel, 2020; Santos *et al.*, 2022; Weyer *et al.*,
98 2019; Van de Weyer *et al.*, 2019). We therefore approached the problem of understanding
99 the underlying genetics of resistance to VSD by building on the structural knowledge of NLR
100 genes and from the progeny QTL studies of Epaina (2012) and Singh (2021). We aimed to
101 leverage the latest sequencing and bioinformatic approaches to gain a clearer insight into the
102 genetic regions of interest. Our premise for the work was that (i) QTLs are informative for
103 predicting resistance, (ii) genetic resistance hotspots are present, (iii) QTLs may indicate the
104 presence of NLR gene clusters, (iv) polymorphic NLR genes within clusters, from contrasting
105 genotypes, may explain disease phenotype. The questions we therefore posed were, can we
106 assemble the cacao genome and successfully discriminate alleles inherited from parents of
107 known VSD phenotype within an F1 tree progeny, and if so, can we determine differences in
108 NLR clusters, type, and specific gene sequences at the QTL locations, based on parentage? An
109 additional question that we tested was, using new sequencing technologies, can we assemble
110 and scaffold to chromosome level both pathogen (~30 Mb) and host (~380 Mb) genomes from
111 a single sample? This would circumvent the inability to culture the biotrophic *C. theobromae*
112 and provide insight into the genomics of a compatible interaction. This final aim was not
113 successful due to the limited pathogen DNA we were able to extract, but future studies could
114 work to improve on this approach.
115 Taking these premises and goals, we built a high-quality parental phased genome resource
116 for a susceptible cacao (clone 26) of known parental cross, **S1 maternal** and **RUQ1347**
117 **paternal**. We annotated the genome for all predicted genes, and then specifically for only
118 NLR-type genes, and conducted fine scale investigation of genomic regions associated with
119 resistance to *C. theobromae* to determine the resistance gene complements inherited from
120 both parents. We made comparative studies into the NLR genes, structurally, quantitatively,
121 and qualitatively. Our investigations show structural differences in NLR presence within
122 parental chromosomes and provide insights into resistance to VSD and potentially other

serious diseases of cacao. Additionally, we provide the first diploid, fully scaffolded and phased genome resource for *Theobroma cacao* L.

Results and Discussion

Near complete parental assigned chromosomes for cultivated *Theobroma cacao*

Using short read sequence data as described in the experimental procedures and github (Tobias, 2024), we assembled and parentally phased the chromosomes of a VSD susceptible *T. cacao* genotype (clone 26) and the progeny of a cross between a VSD resistant (S1) and a VSD susceptible (RUQ1347) genotype. All but one haplotype B (RUQ1347) and two haplotype A (S1) inherited chromosomes shows telomeric caps (black dots in Figure 1). The genomes show few gaps (red plus symbol in Figure 1), high levels of contiguity and completeness, as well as chromosomal synteny (Edwards et al., 2022) based on conserved single copy orthologs (Simão et al., 2015). While some apparent cross-over is visible on chromosomes 4 and 9 (pink synteny lines), these may be biologically real considering the lack of gaps in these assembly regions. The phased genomes are both highly complete according to assessment of conserved single copy orthologs and basic statistics (Table 1).

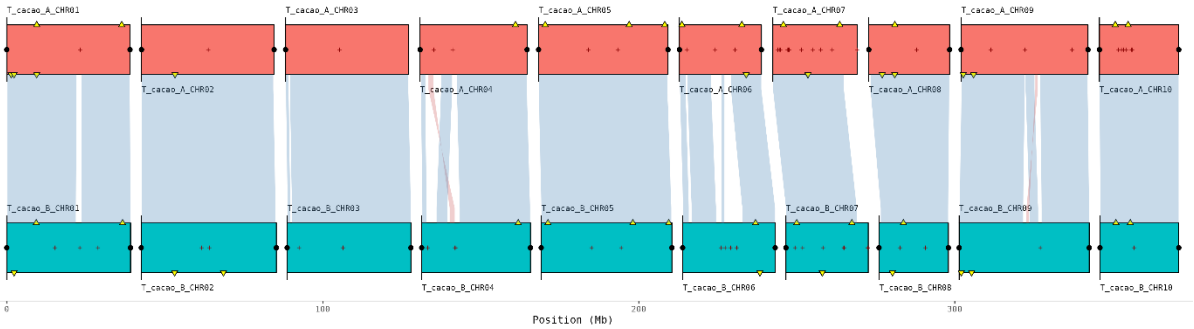

Figure 1 Chromsyn (Edwards et al., 2022) **synteny plots of Theobroma cacao parentally phased genome, haplotype A (top) and B (below). Synteny blocks of collinear "Complete" BUSCO genes** (Simão et al., 2015) **link scaffolds from adjacent assemblies: blue, same strand; red, inverse strand. Yellow triangles mark "Duplicated" BUSCOs. Filled circles mark telomere predictions from Telociraptor (black) (Edwards, 2023). Assembly gaps are marked as dark red + signs.**

The goal for genome assemblies of gapless and telomere-to-telomere (T2T) chromosomes has recently been achievable with the latest sequencing technologies (Sergey et al., 2022). The resulting genome assemblies permit greater depth in understanding structural and evolutionary biology (Mao and Zhang, 2022). Recently, chromosome-level genomes for three wild cacao species from the Upper Amazon were made public (Nousias et al., 2024). These provide the first cacao genomes produced using long read sequence technology and indicate an evolutionary divergence, based on conserved orthologs, from cultivated Criollo and Matina

150 reference genomes (Argout et al., 2011; Motamayor et al., 2013) at ~ 1.83 and ~ 1.34 million
151 years ago. The wild cacao assemblies represent the collapsed haploid state for genomes and
152 are larger in both chromosome and genome base pair (bp) lengths compared with earlier
153 reference genomes. Each of our parentally phased genome assemblies are comparable in size
154 to the wild cacao, at around 380 Mb, however we annotated more predicted protein coding
155 genes at around 26,000 (Table 1) compared to around 21,000, and higher percentage of
156 repetitive sequences at 62% compared to 53% (Nousias et al., 2024). We annotated all genes
157 for the predicted nucleotide binding site (NBARC) domain type as well as predicted 'complete'
158 NLRs that incorporate NBARC plus leucine-rich repeat (LRR) domains (Table 1). Of the
159 complete NLRs we determined only 11 and 15 Toll/Interleukin-1 receptor-type TNL-type, and
160 only 5 and 12 novel integrated domains (ID) within NLRs per haplotype.

161 **Table 1 Raw data statistics from NanoPlot (De Coster and Rademakers, 2023) and genome statistics for both sets of**
162 **parentally inherited *Theombroma cacao* chromosomes using Quast and BUSCOs** (Gurevich et al., 2013; Simão et al., 2015)**.**
163 **Haplotype A chromosomes derived from maternal plant S1 and haplotype B from paternal plant RUQ1347. Annotation**
164 **statistics based on FindPlantNLRs and Funannotate** (Chen et al., 2023; Palmer and Stajich, 2023)**. NLR annotated resistance**
165 **genes were classified and largely conformed to coiled-coil class with only small numbers of Toll/Interleukin-1 receptor-**
166 **type (TIR) and integrated domain type NLRs.**

Raw HiFi data		
Total bases	30,259,224,851	
Mean read length	14,413.4	
Mean read quality	35.6	
Genome statistic	**Haplotype A**	**Haplotype B**
Total genome length (bp)	374,523,129	381,631,648
chromosome length (bp)	338,223,858	340,140,478
No. of chromosomes	10	10
N50 (bp)	38,945,508	39,156,173
L50	5	5
No. of contigs	165	315
GC (%)	33.73	33.67
BUSCO complete (genome; *n* = 1,614)	**98.2%**	**98.4%**
Single-copy	97.5%	97.8%
Duplicated	0.7%	0.6%
BUSCO fragmented	0.6%	0.9%

BUSCO missing	0.3%	0.7%
Protein-coding genes (funannotate)	26,199	26,321
NBARCs (FindPlantNLRs annotation)	342	370
NLRs	293	326
TIR-NLR (TNL)	11	15
Integrated domain (ID) NLRs	5	12
Repeats	**62.0%**	**62.4%**

167 ## Low structural diversity of NLRs between *Theobroma cacao* alleles

168 The NLR-type resistance genes were annotated, as described in the experimental procedures,
169 and the parentally inherited chromosomes were compared, noting that haplotype A (red
170 annotations (Figure 2) aligned with the resistant maternal and haplotype B (yellow
171 annotations) with susceptible paternal trees. We found that the predicted NLR-type genes
172 varied in quantity and types between the two sets of chromosomes. Our research determined
173 a discrepancy of 293 and 326 NLR-type resistance genes within Haplotype A and B
174 respectively. Using the web tool version of OrthoVenn3 (Sun et al., 2023) with the OrthoMLC
175 algorithm, using an expect value of 1e-15 and inflation value 1.5, we found that NLR amino
176 acid sequences clustered into 83 orthologous groups (orthogroups). Of these orthogroups, 82
177 clusters were shared between the two haplotypes with the largest cluster including 55
178 proteins, 28 and 27 from haplotype A and B respectively. Forty-four orthogroups contained a
179 single NLR protein from each haplotype, meaning that the matching homolog was present in
180 each assembly. Nevertheless, aligned sequences for homologous proteins showed some
181 variations and there were also 2.4% single NLRs, numbering 4 and 11 from haplotype A and B
182 respectively.

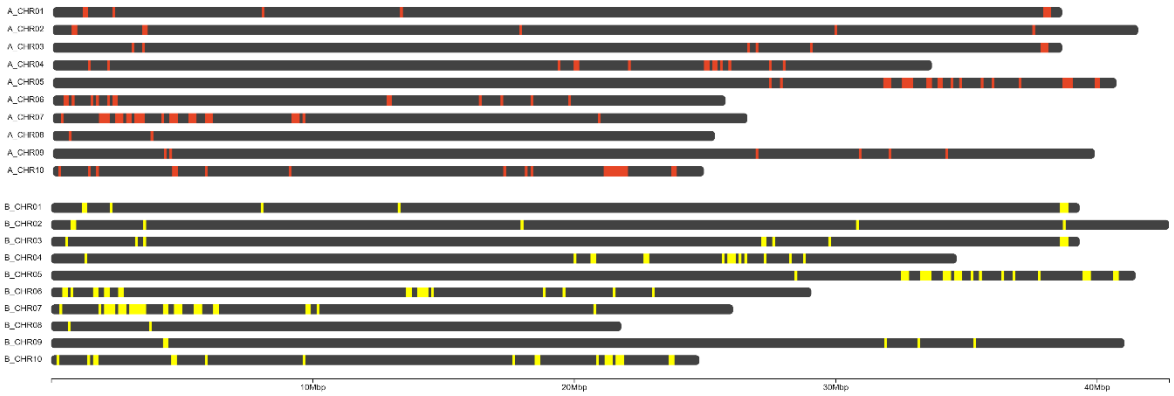

Figure 2 Physical locations of predicted NLR genes on the paired chromosomes of *Theobroma cacao* (A) haplotype A (red) and (B) haplotype B (yellow) generated using ChromoMap (Anand and Rodriguez Lopez, 2022) **in RStudio.**

Low numbers of *Theobroma cacao* NLR-type genes compared to other tree species

Resistance genes of the NLR-type are numerous and highly polymorphic both within and between plant species (Van de Weyer et al., 2019). Trees have generally been shown to have higher numbers of NLR-type genes than herbaceous species, and this is suggested to accomodate a changing pathogen environment over the life of a tree (Tobias and Guest, 2014). More recently, analyses of gene content in diploid genomes have been possible due to advances in sequencing and computational technologies. Notably, tree resistance genes have been investigated within the diploid genome for *Melaleuca quinquenervia* (Chen et al., 2023), highlighting variation in numbers (763 and 733) between haplotypes and across chromosomes for this class of gene. Our analysis of the NLR complement within *T. cacao* showed similar representation to an earlier genome study (Argout et al., 2011) that determined just 297 non-redundant NLR-type genes. Our work, however, presents the diploid content of NLRs at 293 and 326 for haplotype A and B respectively, permitting deeper investigation of homologs at loci. We confirmed low numbers and percentages of the Toll/Interleukin-1 receptor (TIR) NLR class (termed TNLs) of resistance genes within *T. cacao* (Figure 3) compared to many trees within the Rosid clade, in which they comprise 40 - 60% (Arya et al., 2014; Christie et al., 2016; Kohler et al., 2008). This was noted in earlier molecular and genomic studies where only 4% of NLRs contained the TIR domain (Argout et al., 2011; Kuhn et al., 2006), with our classification indicating 3.8% and 5% for haplotype A and B. Unlike the previous study with primers for molecular markers that found TNLs on chromosome three and five (Kuhn et al., 2006), we determined TNLs within clusters on chromosome 4 (three genes), 5 (two genes) and 6 (three and five genes on haplotype A and B), plus a single TNL

208 gene on chromosome 2, 4 and 6 of each haplotype. Our finding of only five and 12 NLR-type
209 genes with non-canonical integrated domains in the two haplotypes also suggests that this
210 integration is less important as a strategy for pathogen recognition and response in cultivated
211 *T. cacao*, compared to other species (Marchal et al., 2022).

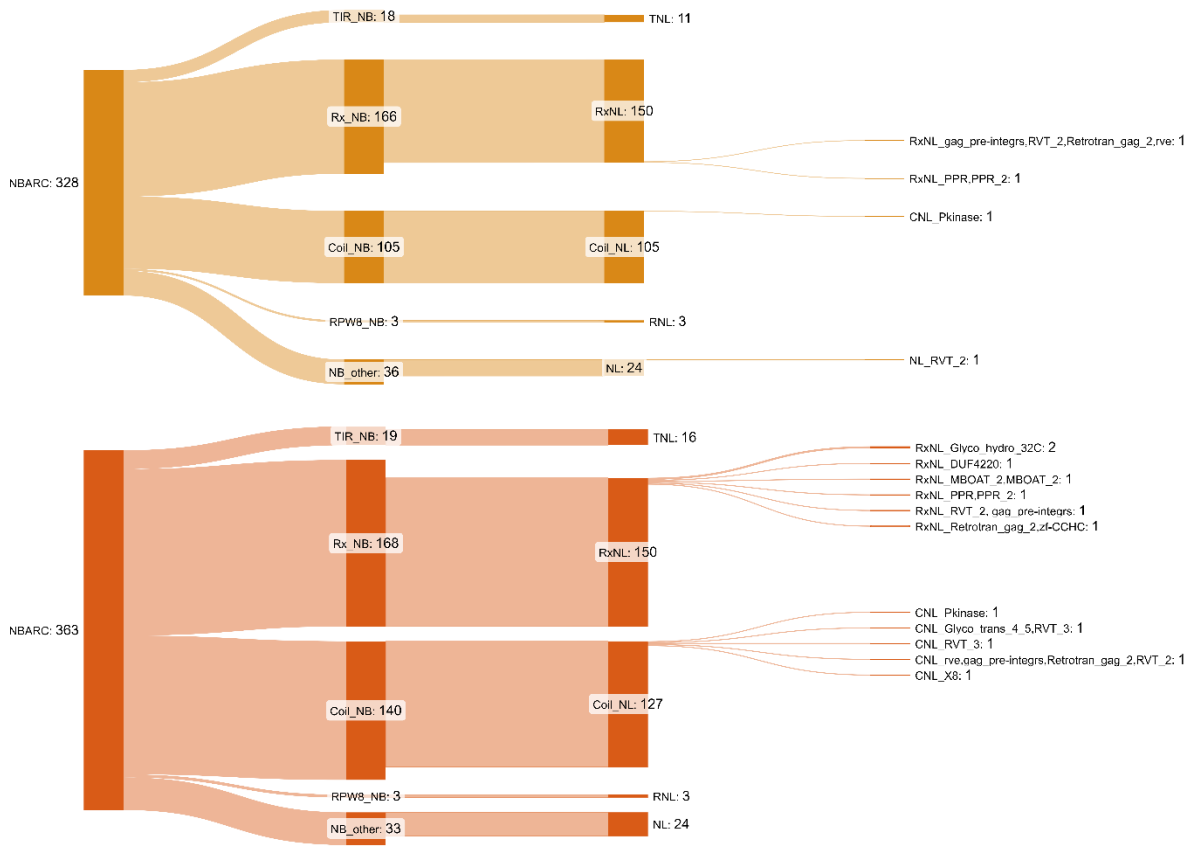

212

213 **Figure 3 The predicted NLR gene complement in the parentally phased *Theobroma cacao* genome. The two sets of**
214 **chromosomes corresponding to (above) Haplotypes A and (below) B were independently classified** (Chen et al., 2023) **and**
215 **visualised to present the domain classes using SankeyMatic (Bogart, 2014) including novel integrated domains (IDs) with**
216 **abbreviations derived from Pfam database** (Mistry et al., 2021)**. NB = Nucleotide Binding Domain, TIR = Toll/Interleukin-1**
217 **receptor, Rx = Potato CC-NB-LRR protein Rx, CC=Coil-Coil Domain, RPW8 = RESISTANCE TO POWDERY MILDEW 8-like**
218 **coiled-coil**

219 *Theobroma cacao* NLR-type genes are present and polymorphic at QTLs for VSD
220 resistance

221 Informative QTL regions were investigated for resistance gene homologs across the parental
222 inherited chromosomes. The most closely aligned VSD QTLs between PNG and Sulawesi *T.*
223 *cacao* progeny trials were on chromosomes 3 and 9, at around 29 and 31 Mb, while
224 chromosome 8 harboured a region between 6 – 7 Mb (Table 3, experimental procedures). We
225 checked these regions based on our annotations for NLRs and identified an NLR cluster of two
226 predicted genes at around 29 Mb on **chromosome 3** within both parentally inherited alleles.

227 The location matches almost exactly with our calculated region based on the reversed start
228 position for the cM QTL (Table 3). When we aligned the four amino acid sequences for these
229 NLRs with ClustalW (Thompson et al., 1994) and visualised in BioEdit (Hall, 1991), we see close
230 homology across the cluster but variation in one haplotype A protein, notably an insertion
231 and deletion in the sequence for gene identity g2391.t1 (Figure 4, above). We found an NLR
232 cluster of three genes on **chromosome 8** at around 3.8 Mb which falls within the 2 cM interval
233 specified by Singh (2021) of 2 - 4 Mb from the QTL locus midpoint. The NLR cluster formed
234 two orthogroups, one group of two head-to-head Rx-NLR predicted proteins from each
235 haplotype (g1318.t1, g1320.t1 and g3681.t1, g3683.t1) and the other of single, nearly exactly
236 homologous proteins, with one amino acid variant, namely proline (g1316.t1, Haplotype A)
237 to arginine (g3679.t1, Haplotype B). Between the region 27 – 36 kb on **chromosome 9** we
238 determined four NLRs from Haplotype A and three from Haplotype B. Paired homologs closest
239 to the calculated QTL mid-point location at around 31 Mb on chromosome nine were aligned
240 and show an insertion/deletion as well as five single amino acid substitutions (Figure 4,
241 below).The single predicted Rx-NLR gene on chromosome 9 of Haplotype A at 27 Mb has no
242 homolog in Haplotype B.
243 The QTLs on chromosome 3 and 8 accounted for 11 and 15% phenotypic variance in the
244 Sulawesi progeny trials and were informative for VSD and PPR resistance in the PNG trial
245 (Table 3). The chromosome 9 QTL accounted for 16 - 18% phenotypic variance in the Sulawesi
246 trial. All putative resistance genes at QTLs were annotated as Rx NLR-type resistance genes.
247 The Rx-NLR coded protein from potato (*Solanum tuberosum*) has been identified as conferring
248 resistance to the potato virus X by direct recognition. Recent work has clarified the interaction
249 of sensor Rx-NLRs with downstream helper NLR protein oligomerisation (Contreras et al.,
250 2023), showing a distinct mechanism for immune responses in plants. While our work has
251 uncovered the arrangement of predicted NLR clusters at QTLs for resistance to VSD,
252 confirmation of these genes is needed across multiple progenies that have clear phenotypes
253 for resistance/susceptibility. Functional validation would also be beneficial to determine
254 mechanisms of recognition and response as it is known that paired head to head NLRs can
255 determine resistance to more than one pathogen (Xi et al., 2022), potentially explaining the
256 results from the study conducted in PNG.

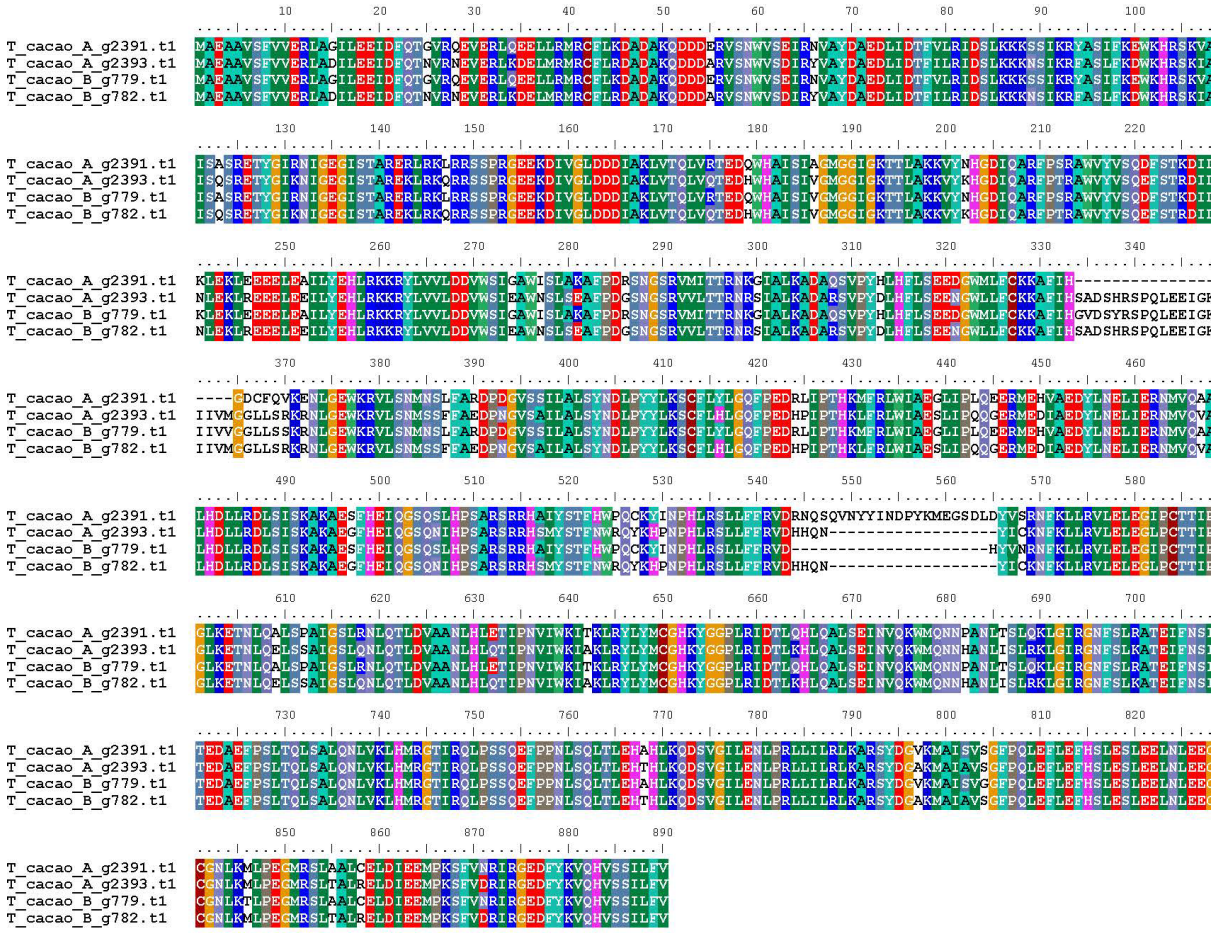
T_cacao_A_g2391.t1
T_cacao_A_g2393.t1
T_cacao_B_g779.t1
T_cacao_B_g782.t1

257

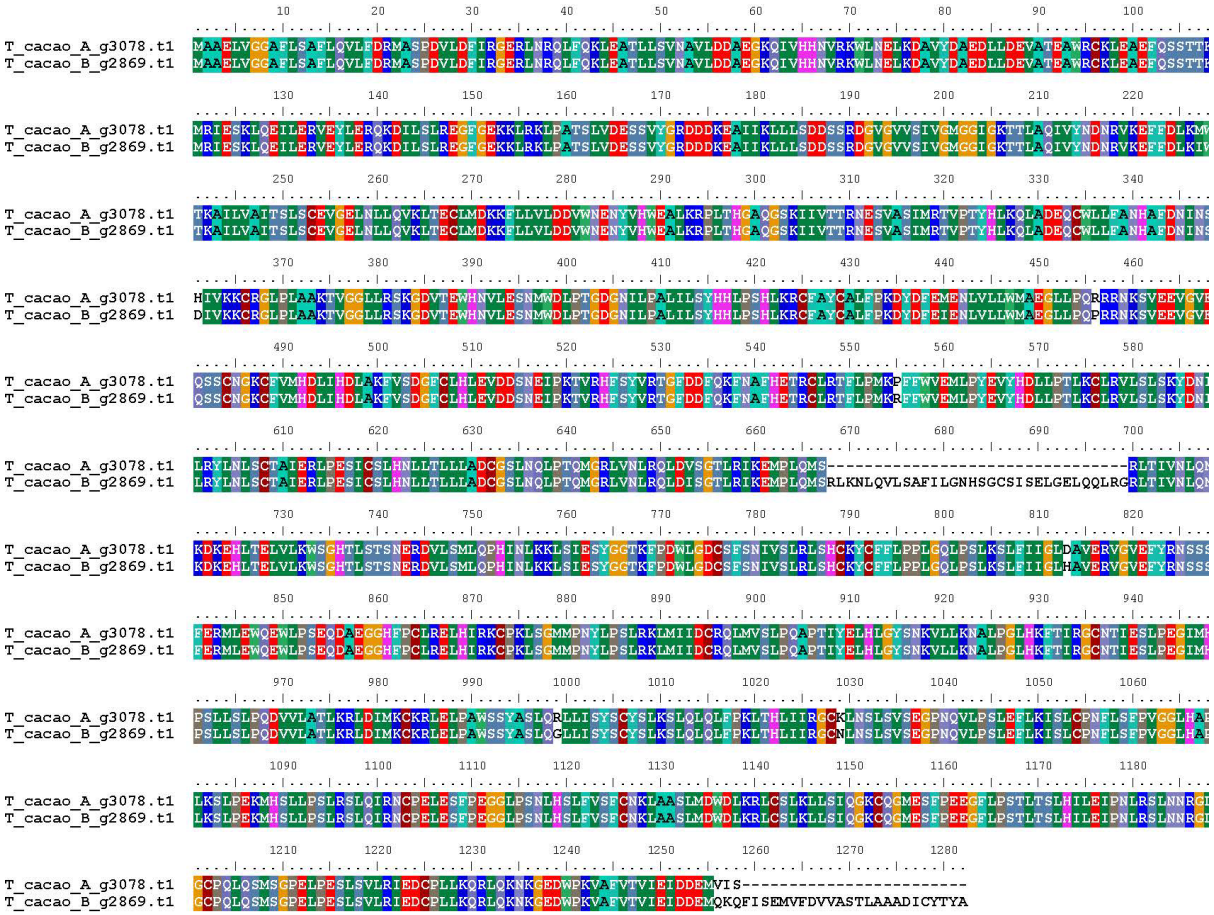

Figure 4 Amino acid sequence alignment of an NLR cluster matching the QTL mapped regions at around 29 Mb on chromosome 3 (above) and single NLR homologs at 31 Mb chromosome 9 (below) within both parentally inherited alleles, A and B, for *Theobroma cacao* clone 26. All predicted NLRs are annotated as Rx-NLRs (Chen et al., 2023) **named for resistance to potato virus X.**

Annotation statistics show high homology between allelic pairs in *Theobroma cacao*

The orthology of all annotated proteins was analysed with OrthoVenn3 as described previously. The predicted proteins indicated 22,486 shared clusters, of which 21,800 included a single predicted homologous gene from each haplotype. The largest cluster had 44 predicted proteins and there were 9.76% singletons. In total there are 2,928 (2,896), 1,865 (1,798), 3,278 (3,315) predicted genes for Haplotype A (and B) on chromosomes 3, 8 and 9 respectively. Except for chromosome 9, with around 76 predicted genes within ~2 Mb of the QTL informing resistance to VSD, the locations on chromosomes 3 and 8 are in highly dense gene-encoding regions, with 325 and 370 predicted genes. We investigated the predicted genes at the QTLs and found that homologs were present between haplotypes (Table 2) and we reviewed their predicted protein functions based on Pfam database (Mistry et al., 2021) annotations. Due to the density of predicted genes, we limited our investigations to

275 immediate proximity around NLRs that corresponded to QTLs. Around the predicted QTL for
276 resistance to VSD on chromosome 3, the Rx-NLR gene cluster is interspersed with two
277 predicted genes coding for protein kinases (Table 2). The kinases have fused LRR domains and
278 predicted transmembrane motifs indicating extracellular receptors and a putative role in
279 defence response. The importance of this class of receptor-like kinase (RLK) has been
280 understood in rice with studies showing *Xa21* confers resistance to *Xanthomonas* sp. and
281 multiple other pathogens (Ercoli et al., 2022). The finding of kinases so closely associated with
282 the Rx-NLR genes on chromosome 3, at the predicted region for VSD resistance QTL, suggests
283 a potential role in disease response and a target for further research. The NLR QTL regions
284 associated with resistance on chromosomes 8 and 9 did not have associated disease
285 response-like genes, however it is likely that multiple genes are involved in the VSD resistance
286 response observed.

287 **Table 2 Predicted and annotated genes that are in proximity to the QTLs for resistance to *Ceratobasium theobromae*,**
288 **causal agent of vascular streak dieback in cultivated *Theobroma cacao*. The annotated genomes are available at NCBI:**
289 **PRJNA1083235 and PRJNA1086984.**

Haplotype A	Haplotype B	Pfam ID	Annotation
NLR QTL chromosome 3 (40 kb region)			
V9T21_008377	WDX93_008321	PF00334	Nucleoside diphosphate kinase
V9T21_008378	WDX93_008322	PF01625	Peptide methionine sulfoxide reductase
V9T21_008380	WDX93_008324	PF07714	Protein tyrosine and serine/threonine kinase
V9T21_008380	WDX93_008324	PF13855	Leucine rich repeat
V9T21_008382	WDX93_008326	PF07714	Protein tyrosine and serine/threonine kinase
V9T21_008382	WDX93_008326	PF13855	Leucine rich repeat
V9T21_008382	WDX93_008326	PF08263	Leucine rich repeat N-terminal domain
V9T21_008383	WDX93_008327	PF02298	Plastocyanin-like domain
NLR QTL chromosome 8 (10 kb region)			
V9T21_020396	WDX93_020310	PF00745	Glutamyl-tRNAGlu reductase, dimerisation domain
V9T21_020396	WDX93_020310	PF01488	Shikimate / quinate 5-dehydrogenase
V9T21_020397	WDX93_020311	PF01293	Phosphoenolpyruvate carboxykinase
V9T21_020399	WDX93_020313	PF08694	Ubiquitin-fold modifier-conjugating enzyme 1
V9T21_020401	WDX93_020315	PF12295	Symplekin tight junction protein C terminal
V9T21_020401	WDX93_020315	PF11935	Symplekin/PTA1 N-terminal
V9T21_020402	WDX93_020316	PF11935	Symplekin/PTA1 N-terminal
V9T21_020404	WDX93_020318	PF00719	Inorganic pyrophosphatase
NLR QTL chromosome 9 (3 kb region)			
V9T21_023576	WDX93_023431	PF00514	Armadillo/beta-catenin-like repeat
V9T21_023578	WDX93_023433	PF02341	RbcX protein
V9T21_023579	WDX93_023434	PF00076	RNA recognition motif

290 ## *Concluding remarks*

291 A recent study, using single nucleotide polymporphisms, confirmed low genetic diversity due
292 to selection for domestication in cultivated cacao (Orduña et al., 2024). The results of that
293 work may explain why similar loci are apparent across varieties for resistance to different
294 diseases, as was found in the two studies, in Indonesia and in PNG, that informed the current
295 research. Genome resources have, until recently, been presented as collapsed haploid
296 genomes and the allocation of QTLs has been limited due to loss of valuable information from
297 the two allele sets. Technologies are rapidly improving and permitting far more detailed
298 comparative studies than were possible only a few years ago.
299 For this research we employed recent advances in technology and software to assemble and
300 assign parental chromosomes for a VSD susceptible *T. cacao* genotype (clone 26) from the
301 Mars Cocoa Research Centre in Pangkep, Sulawesi, Indonesia. We annotated the two parental
302 chromosome sets independently and characterised all the predicted NLR-type resistance
303 genes. The resulting curated and annotated genomes were compared at QTL locations that
304 were identified to explain resistant phenotypes to VSD and PPR. Our results show that the
305 QTLs may indeed resolve to NLR-type resistance genes, and that these may be important to
306 investigate further for breeding trees with resistance to VSD, PPR, and potentially other
307 diseases of cacao. Our work provides a more comprehensive analysis of the predicted NLRs
308 and other genes on each chromosome and shows the variation in structure and type of these
309 genes within a VSD susceptible individual. Future work could develop molecular screening
310 around these specific genes across both resistant and susceptible trees for a range of diseases
311 of cacao. The current work has developed foundational genome resources to facilitate such
312 analyses that may be used to assist future breeding programs for resistance.

313 ## *Experimental procedures*

314 ### High Molecular Weight DNA extraction protocol testing

315 Prior to our work in Sulawesi, Indonesia, we ran exhaustive high molecular weight (HMW)
316 DNA extraction protocol testing on cacao leaf samples from plants maintained in the
317 University of Sydney greenhouses. A persistent problem remained for clean extractions due
318 to high contaminant levels that had the properties of a jelly-like substance, presumably
319 pectin, though not confirmed. We attempted to resolve the nature of the contaminant with

enzymatic testing using pectinase. We also tested our contaminant DNA with nuclear magnetic resonance spectrometer (NMR). Data was collected on a 600 MHz spectrometer equipped with triple resonance CryopProbe and the following buffer conditions: 10 mM Tris; 10% D2O; pH 8.0, in 3 mm short NMR tubes (volume ~160 µl). We ran controls of 10 mM Tris buffer and clean HMW DNA in Tris buffer. Test samples included pectin, pectin with pectinase treatment, contaminated DNA with pectinase treatment, contaminated DNA with macerozyme (incl. pectinase) treatment. Unfortunately the signals in the aromatic/amide regions were beyond detection, suggesting a large DNA-contaminant (potentially covalent) complex form in this sample. Young leaves were found to produce cleaner DNA but did not show any symptoms of VSD, so we aimed to extract samples from older infected leaves using a combined protocol described below that improved on but did not resolve the contaminant problem.

Cacao leaf material collected from field trial tree

We collected fully expanded leaf material on the 10 January 2023, during wet weather, from the Mars Cocoa Research Institute field trials in Pangkep, South Sulawesi, Indonesia. The leaves were found on T. *cacao* F1 generation progeny, VSD susceptible clone number 26, from Sulawesi 1 – S1 (resistant maternal), crossed with RUQ 1347 (MIS_GBR207_CCN 51) (susceptible paternal) parental plants (Turnbull et al., 2017). The leaves were symptomatic of VSD with browning of the leaf apex and vascular death visible in the petiole (Figure 5). Leaves were placed in plastic bags and transported to the laboratories at Universitas Hasannudin, Makassar and refrigerated overnight.

Figure 5 Leaf from Theobroma cacao, VSD susceptible clone 26, growing at the Mars Cocoa Research Institute field trials, Pangkep South Sulawesi, Indonesia. (Left) The symptomatic leaf apex dieback and some chlorosis indicating Ceratobasium theobromae. (Right) Visible vascular death caused by the pathogen. Scale bar left ~5 cm.

345 ## High Molecular Weight DNA extracted from cacao leaves

346 The following day while leaves were fresh, HMW DNA was extracted using a protocol adapted
347 from the sorbitol wash method developed by Jones et al. (2021), and the HMW plant DNA
348 CTAB extraction method developed by Hilario (2018). Small (1 cm^2) pieces of the leaves were
349 placed into 1.5 mL centrifuge tubes with a small amount (a few mg) of PVP40000. The tissue
350 was flash frozen in liquid nitrogen and ground into a powder with micropestle while frozen.
351 Three or more rounds of sorbitol wash were used on the samples, in accordance with the
352 protocol (Jones et al., 2021), until the supernatant was no longer viscous. Then DNA was
353 extracted, according to the protocol (Hilario, 2018), using CTAB buffer with an incubation step
354 at 56 °C for 2 hours, in a water bath. Apart from an extended RNase A incubation step, of 10
355 mins, the protocol was followed until the precipitation step. The DNA formed a visible
356 gelatinous precipitate at this stage and was left to continue precipitating at -20 °C overnight.
357 The following day the DNA was collected by centrifugation at 3000 rpm for 25 min at room
358 temperature and cleanup steps followed according to the protocol before dissolving in 10
359 mM Tris-HCL pH 8.0. The DNA was quantified, and purity was checked using a NanoDrop™
360 Lite Plus spectrophotometer and a QuBit™ 2.0 Fluorometer. Purified HMW DNA (10 x 1.5 µL
361 tubes) was couriered under an Australian Department of Agriculture, Water, and the
362 Environment import permit to the Australian Genome Research Facility (AGRF), Brisbane,
363 Australia, for cleanup, size selection, library prep and sequencing on Pacific Biosciences of
364 California, Inc. (PacBio) Sequel II.

365 ## Formaldehyde cross-linking of leaves for HiC sequencing

366 We prepared samples according to the manufacturer's protocols for chromatin crosslinking
367 library prep and sequencing at Phase Genomics (Seattle, Washington, US) to obtain HiC reads.
368 Five grams of leaf material was immersed in 2% (v/v) sodium hypochlorite for 2 mins for
369 surface sterilisation and then washed with ultrapure water. The leaves were cut into strips
370 and immersed in 1% (v/v) formaldehyde for 40 minutes with intermittent mixing. The
371 crosslinking reaction was quenched with the addition of glycine to a final concentration of
372 125 mM for 15 minutes. The crosslinked leaves were washed with ultrapure water, dried,
373 then ground to a powder after freezing with liquid nitrogen.

374 ## Data processing and genome assembly

375 Details of all the software, versions, parameters and scripts used to process the data are
376 available here: https://github.com/peritob/Theobroma-cacao-genome/tree/main

377 ## Preparing the raw data for processing

378 We downloaded the 23 GB (ccs.bam) HiFi sequence read data from AGRF, filtered the reads
379 using HiFiAdapterFilt (Sim et al., 2022) and checked the statistics using Nanoplot (De Coster
380 and Rademakers, 2023). The HiC paired-end read (25 GB) mapping statistics against the cacao
381 Criollo reference genome (GCF_000208745.1) were good for informative read pairs (12.18%)
382 but not against the pathogen genome (GCA_012932095.1) at (0.03%), although 4.28% same
383 strand high quality reads were mapped. We mapped all the filtered HiFi reads to the *C.*
384 *theobromae* genome (Ali et al., 2019) with Minimap2 (Li, 2018) to filter the pathogen from
385 host. We presumed all the mapped reads to be pathogen and all the unmapped reads to be
386 from the host and proceeded accordingly. Additionally, we ran a local blast with internal
387 transcribed spacer (ITS) primers on the VSD mapped raw sequence reads. This confirmed a
388 single exact *in silico* hit using the ITS regions using forward primers ITS4 (White et al., 1990)
389 and reverse ITS5A (Stanford et al., 2000). Raw Illumina data available for the parental plants
390 was trimmed of adaptors and low quality reads with Fastp (Chen et al., 2018).

391 ## Genome assembly and chromosome scaffolding

392 We attempted several assembly approaches with Hifiasm software (Cheng et al., 2021).
393 Previous experience with HiC scaffolding has shown the possibility to phase the separate
394 nuclear compartments (Tobias et al., 2022). We therefore attempted to build a plant-
395 pathogen hybrid genome to scaffold with HiC and visually identify and separate the two
396 organisms using the heatmaps. The hybrid genome did not complete, likely due to insufficient
397 overlaps for the pathogen reads. We tried to assemble all the pathogen reads into consensus
398 sequences using Flye (Kolmogorov et al., 2019) and Hifiasm without success. We then tested
399 the trio-binning option for Hifiasm of the diploid *T. cacao* incorporating the Illumina parental
400 reads after running Yak (Li, 2020). This was unsuccessful, so we assembled the diploid *T. cacao*
401 genome using HiC integration with Hifiasm followed by HiC scaffolding of the resulting
402 genomes independently with Juicer (Neva C. Durand et al., 2016), 3D-DNA (Dudchenko et al.,
403 2017) and manual scaffolding with Juicebox (Neva C Durand et al., 2016).

404 *Theobroma cacao* genome curation

405 We used the Matina 1-6 cacao genome (GCF_000403535.1) to anchor our genome scaffolds
406 with PAFScaff (Field et al., 2020) based on Minimap2 (Li, 2018) mapping. We screened the
407 resulting fasta files for non-nuclear genomic contaminants with FCS-GX (Astashyn et al., 2024)
408 and Tiara (Karlicki et al., 2022). In each case, the two haplotypes were run independently.
409 FCS-GX was run against the NCBI gxdb (build date 2023-01-24; downloaded 2023-09-12).
410 Additional checks of contamination were executed with Taxolotl (Tobias et al., 2022). Taxolotl
411 was provided with the annotation for each haplotype and run with taxwarnrank=class using
412 mmseqs2 against the NCBI nr database (compiled 2022-05-19). In addition to generating
413 results for all sequences in each haplotype, analysis of subsets was performed for (1)
414 chromosome scaffolds only, (2) pure FCS-GX scaffolds, (3) contaminated FCS-GX scaffolds, (4)
415 Tiara "eukarya" scaffolds, and (5) scaffolds not classified as "eukarya" by Tiara. Results were
416 visualised with Pavian. Lists were made of non-plant contaminant contigs from the
417 fcs_gx_reports and were removed, as well as plastid contigs flagged in the tiara outputs. We
418 then ran Telociraptor (Edwards, 2023) followed by Chromsyn (Edwards et al., 2022) on the
419 chromosome-level contigs to compare synteny and manually adjusted according to the contig
420 graphs and figure outputs. We used the parental data available within our lab (Singh, 2021)
421 to assign scaffolds and contigs. We mapped the maternal S1 data to the concatenated
422 haplotype A and B genomes using Hisat2 (Kim et al., 2019) and then similarly mapped the
423 RUQ1347 data. We assumed that the most reads mapped were the likely parental
424 chromosome/contig and curated each genome. Of the chromosomes, 3, 5 and 8 were
425 switched accordingly (Figure 6). We designated the S1 maternally inherited contigs as genome
426 T_cacao_v1.3_A, and RUQ1347 paternally inherited as T_cacao_v1.3_B.

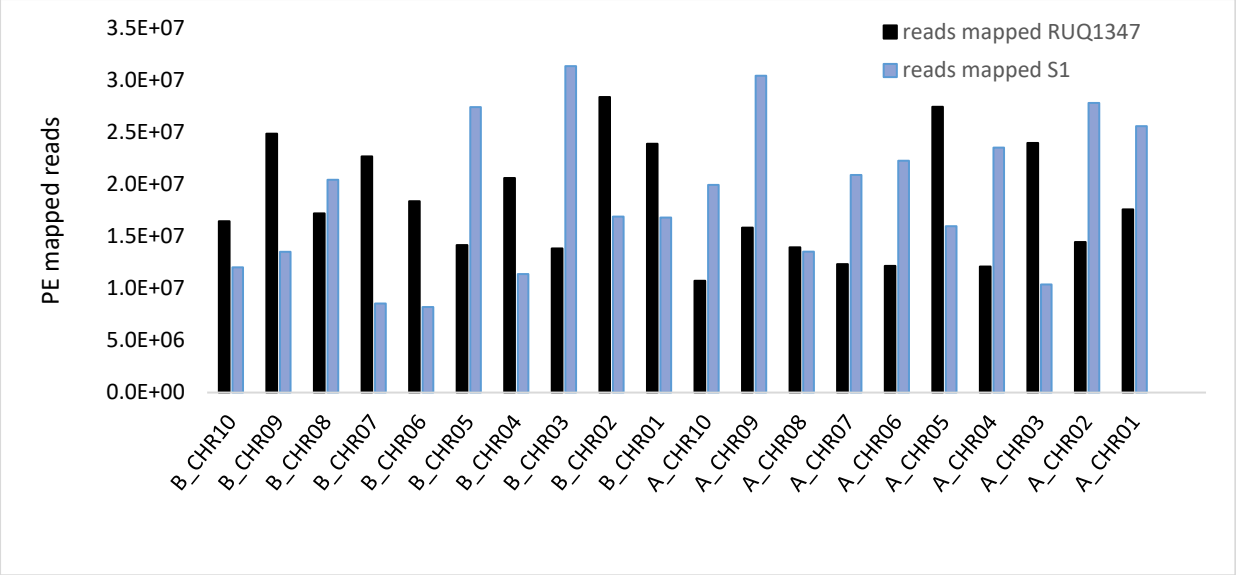

Figure 6 Theobroma cacao resistant (S1) and susceptible (RUQ1347) parental paired-end (PE) Illumina sequence reads mapped to the concatenated Hap A and B progeny chromosomes. The reads that were mapped in greater numbers to chromosomes and contigs were used to determine parental assignment and swapped accordingly.

Parental assigned genomes were annotated independently

To repeat mask the genome for annotation we ran both genomes through Repeatmasker and Repeatmodeler. We then mapped publicly available RNAseq data from CCN51 *Theobroma cacao* from NCBI (PRJNA933172) to the soft-masked genomes independently with hisat2. We trimmed the RNAseq data with Fastp (Chen et al., 2018) prior to mapping and processed the outputs with Samtools (Li et al., 2009) to make bam files. The mapped RNAseq bam files were used as evidence to predict protein coding genes within the funannotate (Palmer and Stajich, 2023) *predict* pipeline with the BUSCO embryophyte (Manni et al., 2021; Simão et al., 2015) database. We used Interproscan5 (Jones et al., 2014) independently and then ran funannotate *annotate* to obtain final predicted proteins and coding sequences. In order to make GenBank (Sayers et al., 2023) compatible annotations, we ran the resulting files with Table2asn (GenBank, 2023).

NLR-type resistance gene annotation

We annotated the resistance gene complement with the FindPlantNLRs pipeline (Chen et al., 2023), that incorporates NLR-Annotator (Steuernagel et al., 2020), HMMER (Finn et al., 2015; Johnson et al., 2010) and BLAST (Altschul et al., 1990) components as well as Interproscan5 (Jones et al., 2014). Unlike many annotation methods, the pipeline takes an unmasked genome as a starting point to avoid masking, and hence not annotating, repetitive LRR regions

449 that are characteristic of NLR-type genes. The last stage of the pipeline determines NLR gene
450 classes, including predicted integrated domains, and locations within each parental
451 haplotype. All NLRs were plotted to visualise on chromosomes with Chromomap (Anand and
452 Rodriguez Lopez, 2022) and classes, based on domain Pfams, were visualised with
453 Sankeymatic (Bogart, 2014).

454 QTL locations on chromosomes predicted and compared against NLR-type gene 455 predictions

456 Informative QTLs for resistance to VSD were obtained from data of two previous studies
457 (Epaina, 2012; Singh, 2021). Using the chromosome lengths for our parental genome
458 haplotypes we calculated the predicted locations for VSD resistance QTLs. In brief, we took
459 averages of Linkage Group (LG) map lengths (Epaina, 2012), and divided the chromosome
460 base pair length from assembled genomes (current study) by centimorgan (cM). We then
461 determined the expected mid-point (in base pairs) for the resistance QTLs. Singh (2021)
462 predicted QTLs confidence intervals at 3-4 Mb and determined three significant QTLs; on
463 chromosome 3, 8 and 9. Initially our calculations for the QTL locations from the PNG progeny
464 study showed a significant region at around 18.5 Mb on chromosome 8 (Table 2). This was
465 not concordant with the Sulawesi study, at between 5.5 and 8.8 Mb, leading us to investigate
466 if our calculations were misrepresenting the 'start' position for chromosome eight. When
467 recalculated based on the reverse orientation, we found that the QTL matched more closely,
468 at around 7 Mb. We also noted that the QTL identified on chromosome 3, when start positions
469 were reversed, indicated a cluster of NLR-type genes at around 30 Kb. Several significant QTLs
470 were associated with resistance to other pathogens including PPR (Table 2) in the study by
471 Epaina (2012). QTLs that were in similar regions within both studies were regarded as likely
472 harbouring useful candidate genes for breeding resistance. The most closely aligned VSD QTLs
473 between studies were on chromosomes 3, 8 and 9. Detailed comparisons for the VSD
474 significant QTLs across the two studies were undertaken to investigate resistance gene
475 homologs and other predicted genes across the parental chromosomes.

Table 3 QTLs for vascular streak dieback (VSD) resistance were calculated using average *Theobroma cacao* Linkage Group (LG) lengths (Epaina, 2012) and dividing chromosome lengths (bp) by LG lengths (in cM) to determine 1 cM in bp (per chromosome). QTLs (cM) were then multiplied by bp length for 1 cM to obtain the chromosome locations for the diploid genome. Green cells and brown cells are VSD and *Phytophthora* pod rot (PPR) resistance QTL physical locations on chromosomes.

***Theobroma cacao* A (S1 inherited)**											
Chromosomes (LG)		**1**	**2**	**3**	**4**	**5**	**6**	**7**	**8**	**9**	**10**
cM (average)		99.9	107.2	91.6	79.7	89.8	75.8	56.6	60	106.1	62.4
bp per chromosome (this study)		39,005,981	41,965,441	38,945,508	33,857,508	40,959,067	25,938,454	26,721,266	25,579,687	40,159,845	25,091,101
bp per cM		390,450	391,469	425,169	424,812	456,114	342,196	472,107	426,328	378,509	402,101
Singh (2021)	VSD QTL (bp)			9,353,725 **(*29,591,783)**					8,782,359	25,170,874	
Epaina (2012)	VSD QTL (bp)	11,270,737	26,861,405	8,531,872 **(*30,413,636)**	27,163,747	7,976,071			18,514,151 **(*7,065,536)**	31,452,994	
Epaina (2012)	PPR QTL (bp)			8,531,872 **(*30,413,636)**	23,158,620	6,937,499			18,514,151 **(*7065,536)**		
***Theobroma cacao* B (RUQ1347 inherited)**											
Chromosomes (LG)		**1**	**2**	**3**	**4**	**5**	**6**	**7**	**8**	**9**	**10**
bp per chromosome (this study)		39,156,173	42,761,000	39,170,102	34,430,140	41,360,500	29,284,707	25,927,970	21,951,902	41,168,245	24,929,739
bp per cM		391,954	398,890	427,621	431,997	460,585	386,342	458,091	365,865	388,014	399,515
Singh (2021)	VSD QTL (bp)			9,407,666 **(*29,762,436)**					7,536,820	25,802,906	
Epaina (2012)	VSD QTL (bp)	11,314,135	27,370,630	8,581,075 **(*30,589,027)**	27,623,167	8,054,243			15,888,421 **(*6,063,481)**	32,242,768	
Epaina (2012)	PPR QTL (bp)			8,581,075 **(*30,589,027)**	23,550,302	7,005,492			15,888,421 **(*6,063,481)**		

***QTL determined with start position on chromosome reversed.**

Acknowledgements

The Joint Cocoa Research Fund, European Cocoa Association contributed funds to support this research. The authors acknowledge the facilities, and the scientific and technical assistance of the Sydney Informatics Hub at the University of Sydney and, in particular, access to the high-performance computing facility Artemis. We acknowledge the support of Sydney Analytical for running samples and interpretation on the University of Sydney Nuclear Magnetic Resonance (NMR) Core Facilities. Thank you to Mark Powrie who generously assisted during the work in Sulawesi.

Author contributions

DG and PT initiated and led the project. PT and JD collected the material from established clonal trials developed and managed by AP. JM and AP supported and facilitated the research in Sulawesi. JD, PT, AZ, EB extracted HMW DNA and cross-linked samples. PT and EB organised sample deliveries. PE and GS provided results of QTL trials that were supported by DG and RP. GS provided parental data. PT assembled, curated, annotated the genomes, and interpreted results, RE ran contamination screening of genomes. PT submitted the data to NCBI and wrote the manuscript. All authors contributed comments and edits to the manuscript.

Data availability statement

All data that support the findings of this research are publicly available. Raw data is available at National Centre for Biotechnology Information (NCBI) under the following biosample accession: SAMN40241783 and bioproject accession: PRJNA1083235. Annotated diploid *Theobromae cacao* (clone 26) genomes are available here: PRJNA1083235 (maternally inherited), PRJNA1086984 (paternally inherited). NLR predicted coding and amino acid sequences and gff3 data is available at https://github.com/peritob/Theobroma-cacao-genome/tree/main.

References

Ali, S.S., Asman, A., Shao, J., Firmansyah, A.P., Susilo, A.W., Rosmana, A., et al. (2019) Draft genome sequence of fastidious pathogen Ceratobasidium theobromae, which causes vascular-streak dieback in Theobroma cacao. *Fungal Biology and Biotechnology*, 6, 1–10. https://doi.org/10.1186/s40694-019-0077-6.

Altschul, S.F., Gish, W., Miller, W., Myers, E.W. & Lipman, D.J. (1990) Basic local alignment

search tool. *Journal of molecular biology*, 215, 403–10. https://doi.org/10.1016/S0022-2836(05)80360-2.

Anand, L. & Rodriguez Lopez, C.M. (2022) ChromoMap: an R package for interactive visualization of multi-omics data and annotation of chromosomes. *BMC Bioinformatics*, 23, 1–9. https://doi.org/10.1186/s12859-021-04556-z.

Argout, X., Salse, J., Aury, J.-M., Guiltinan, M.J., Droc, G., Gouzy, J., et al. (2011) The genome of Theobroma cacao. *Nature genetics*, 43, 101–108. https://doi.org/10.1038/ng.736.

Arya, P., Kumar, G., Acharya, V. & Singh, A.K. (2014) Genome-wide identification and expression analysis of NBS-encoding genes in *Malus* x *domestica* and expansion of *NBS* genes family in Rosaceae. *PloS one*, 9, e107987. https://doi.org/10.1371/journal.pone.0107987.

Astashyn, A., Tvedte, E.S., Sweeney, D., Sapojnikov, V., Bouk, N., Joukov, V., et al. (2024) Rapid and sensitive detection of genome contamination at scale with FCS-GX. *Genome Biology*, 25, 1–25. https://doi.org/10.1186/s13059-024-03198-7.

Bailey, B.A. & Meinhardt, L.W. eds. (2016) Cacao Diseases: A History of Old Enemies and New Encounters. Cacao Diseases: A History of Old Enemies and New Encounters. Heidelberg: Springer International Publishing.

Barragan, A.C. & Weigel, D. (2020) Plant NLR Diversity : The Known Unknowns of Pan-NLRomes A Brief History of Plant NLRs. *The Plant Cell*.

Bhunjun, C.S., Phillips, A.J.L., Jayawardena, R.S., Promputtha, I. & Hyde, K.D. (2021) Importance of molecular data to identify fungal plant pathogens and guidelines for pathogenicity testing based on Koch'S postulates. *Pathogens*, 10, 1–18. https://doi.org/10.3390/pathogens10091096.

Bogart, S. (2014) SankeyMatic. https://sankeymatic.com/build/

Chen, S., Zhou, Y., Chen, Y. & Gu, J. (2018) Fastp: An ultra-fast all-in-one FASTQ preprocessor. *Bioinformatics*, 34, i884–i890. https://doi.org/10.1093/bioinformatics/bty560.

Chen, S.H., Martino, A.M., Luo, Z., Schwessinger, B., Jones, A., Tolessa, T., et al. (2023) A high-quality pseudo-phased genome for Melaleuca quinquenervia shows allelic diversity of NLR-type resistance genes. *GigaScience*, 12, 1–18. https://doi.org/10.1093/gigascience/giad102.

Cheng, H., Concepcion, G.T., Feng, X., Zhang, H. & Li, H. (2021) Haplotype-resolved de novo assembly using phased assembly graphs with hifiasm. *Nature Methods*, 18, 170–175. https://doi.org/10.1038/s41592-020-01056-5.

Christie, N., Tobias, P.A., Naidoo, S. & Külheim, C. (2016) The *Eucalyptus grandis NBS-LRR* gene family: physical clustering and expression hotspots. *Frontiers in Plant Science*, 6, 1–16. https://doi.org/10.3389/fpls.2015.01238.

Contreras, M.P., Pai, H., Tumtas, Y., Duggan, C., Yuen, E.L.H., Cruces, A.V., et al. (2023) Sensor NLR immune proteins activate oligomerization of their NRC helpers in response to plant pathogens . *The EMBO Journal*, 42. https://doi.org/10.15252/embj.2022111519.

Coster, W. De & Rademakers, R. (2023) NanoPack2: population-scale evaluation of long-read sequencing data. *Bioinformatics*, 39, 0–2. https://doi.org/10.1093/bioinformatics/btad311.

Daymond, A.J., Mendez, D.G., Hadley, P., Bastide, P., Abdoellah, S., Acheampong, K., et al. (2022) *A Global Review of Cocoa Farming Systems*.

Dudchenko, O., Batra, S.S., Omer, A.D., Nyquist, S.K., Hoeger, M., Durand, N.C., et al. (2017) De novo assembly of the Aedes aegypti genome using Hi-C yields chromosome-length scaffolds. *Science*, 356, 92–95. https://doi.org/10.1126/science.aal3327.

557 Durand, Neva C, Robinson, J.T., Shamim, M.S., Machol, I., Mesirov, J.P., Lander, E.S., et al.
558 (2016) Juicebox Provides a Visualization System for Hi-C Contact Maps with Unlimited
559 Zoom Tool. *Cell Systems*, 3, 99–101. https://doi.org/10.1016/j.cels.2015.07.012.
560 Durand, Neva C., Shamim, M.S., Machol, I., Rao, S.S.P., Huntley, M.H., Lander, E.S., et al.
561 (2016) Juicer Provides a One-Click System for Analyzing Loop-Resolution Hi-C
562 Experiments. *Cell Systems*, 3, 95–98. https://doi.org/10.1016/j.cels.2016.07.002.
563 Edwards, R.J. (2023) Telociraptor. https://github.com/slimsuite/telociraptor/tree/main
564 Edwards, R.J., Dong, C., Park, R.F. & Tobias, P.A. (2022) A phased chromosome-level genome
565 and full mitochondrial sequence for the dikaryotic myrtle rust pathogen, Austropuccinia
566 psidii. *bioRxiv*, 2022.04.22.489119. https://doi.org/10.1101/2022.04.22.489119.
567 Epaina, P. (2012) *Identification of Molecular Markers and Quantitative Trait Loci linked to*
568 *resistance to Vascular Streak Dieback and Phytophthora Pod Rot of Cacao (Theobroma*
569 *cacao L .)*. The University of Sydney.
570 Ercoli, M.F., Luu, D.D., Rim, E.Y., Shigenaga, A., Araujo, A.T. de, Chern, M., et al. (2022) Plant
571 immunity: Rice XA21-mediated resistance to bacterial infection. *Proceedings of the*
572 *National Academy of Sciences of the United States of America*, 119.
573 https://doi.org/10.1073/pnas.2121568119.
574 Field, M.A., Rosen, B.D., Dudchenko, O., Chan, E.K.F., Minoche, A.E., Edwards, R.J., et al.
575 (2020) Canfam-GSD: De novo chromosome-length genome assembly of the German
576 Shepherd Dog (Canis lupus familiaris) using a combination of long reads, optical
577 mapping, and Hi-C. *GigaScience*, 9, 1–12. https://doi.org/10.1093/gigascience/giaa027.
578 Finn, R.D., Clements, J., Arndt, W., Miller, B.L., Wheeler, T.J., Schreiber, F., et al. (2015)
579 HMMER web server: 2015 Update. *Nucleic Acids Research*, 43, W30–W38.
580 https://doi.org/10.1093/nar/gkv397.
581 Fluhr, R., King, S.I., Vi, H. & Shakespeare, W. (2001) Sentinels of Disease . Plant Resistance
582 Genes. 127, 1367–1374. https://doi.org/10.1104/pp.010763.1.
583 GenBank (2023) Table2asn. https://www.ncbi.nlm.nih.gov/genbank/table2asn/
584 Guest, D. & Keane, P. (2007) Vascular-streak dieback: A new encounter disease of cacao in
585 Papua New Guinea and Southeast Asia caused by the obligate basidiomycete
586 Oncobasidium theobromae. *Phytopathology*, 97, 1654–1657.
587 https://doi.org/10.1094/PHYTO-97-12-1654.
588 Gurevich, A., Saveliev, V., Vyahhi, N. & Tesler, G. (2013) QUAST: Quality assessment tool for
589 genome assemblies. *Bioinformatics*, 29, 1072–1075.
590 https://doi.org/10.1093/bioinformatics/btt086.
591 Hall, T.A. (1991) BioEdit: a user-friendly biological sequence alignment editor and analysis
592 program for Windows 95/98/NT. *Nucleic Acids Symposium Series*, 41, 95–98.
593 Hilario, E. (2018) Plant nuclear genomic DNA preps. *protocols.io:*
594 Johnson, L.S., Eddy, S.R. & Portugaly, E. (2010) Hidden Markov model speed heuristic and
595 iterative HMM search procedure. *BMC Bioinformatics*, 11.
596 https://doi.org/10.1186/1471-2105-11-431.
597 Jones, A., Torkel, C., Stanley, D., Nasim, J., Borevitz, J. & Schwessinger, B. (2021) High-
598 molecular weight DNA extraction, cleanup and size selection for long-read sequencing.
599 *PLoS ONE*, 16, 1–6. https://doi.org/10.1371/journal.pone.0253830.
600 Jones, P., Binns, D., Chang, H.Y., Fraser, M., Li, W., McAnulla, C., et al. (2014) InterProScan 5:
601 Genome-scale protein function classification. *Bioinformatics*, 30, 1236–1240.
602 https://doi.org/10.1093/bioinformatics/btu031.
603 Junaid, M., Purwantara, A. & Guest, D. (2020) First report of vascular streak dieback symptom

of cocoa caused by Ceratobasidium theobromae in Barru District, South Sulawesi. *IOP Conference Series: Earth and Environmental Science*, 486. https://doi.org/10.1088/1755-1315/486/1/012170.

Karlicki, M., Antonowicz, S. & Karnkowska, A. (2022) Tiara: deep learning-based classification system for eukaryotic sequences. *Bioinformatics*, 38, 344–350. https://doi.org/10.1093/bioinformatics/btab672.

Keane, P.J., Flentje, N.J. & Lamb, K.P. (1972) Investigation of vascular-streak dieback of cocoa in papua new guinea. *Australian Journal of Biological Sciences*, 25, 553–564. https://doi.org/10.1071/BI9720553.

Kim, D., Paggi, J.M., Park, C., Bennett, C. & Salzberg, S.L. (2019) Graph-based genome alignment and genotyping with HISAT2 and HISAT-genotype. *Nature Biotechnology*, 37, 907–915. https://doi.org/10.1038/s41587-019-0201-4.

Kohler, A., Rinaldi, C., Duplessis, S., Baucher, M., Geelen, D., Duchaussoy, F., et al. (2008) Genome-wide identification of NBS resistance genes in Populus trichocarpa. *Plant Molecular Biology*, 66, 619–636. https://doi.org/10.1007/s11103-008-9293-9.

Kolmogorov, M., Yuan, J., Lin, Y. & Pevzner, P.A. (2019) Assembly of long, error-prone reads using repeat graphs. *Nature Biotechnology*, 37, 540–546. https://doi.org/10.1038/s41587-019-0072-8.

Kuhn, D.N., Narasimhan, G., Nakamura, K., Brown, J.S., Schnell, R.J. & Meerow, A.W. (2006) Identification of cacao TIR-NBS-LRR resistance gene homologues and their use as genetic markers. *Journal of the American Society for Horticultural Science*, 131, 806–813. https://doi.org/10.21273/jashs.131.6.806.

Lanaud, C., Fouet, O., Clément, D., Boccara, M., Risterucci, A.M., Surujdeo-Maharaj, S., et al. (2009) A meta-QTL analysis of disease resistance traits of Theobroma cacao L. *Molecular Breeding*, 24, 361–374. https://doi.org/10.1007/s11032-009-9297-4.

Li, H. (2018) Minimap2: Pairwise alignment for nucleotide sequences. *Bioinformatics*, 34, 3094–3100. https://doi.org/10.1093/bioinformatics/bty191.

Li, H. (2020) Yak. https://github.com/lh3/yak/releases/tag/v0.1

Li, H., Handsaker, B., Wysoker, A., Fennell, T., Ruan, J., Homer, N., et al. (2009) The Sequence Alignment/Map format and SAMtools. *Bioinformatics*, 25, 2078–2079. https://doi.org/10.1093/bioinformatics/btp352.

Manni, M., Berkeley, M.R., Seppey, M., Simão, F.A. & Zdobnov, E.M. (2021) BUSCO Update: Novel and Streamlined Workflows along with Broader and Deeper Phylogenetic Coverage for Scoring of Eukaryotic, Prokaryotic, and Viral Genomes. *Molecular Biology and Evolution*, 38, 4647–4654. https://doi.org/10.1093/molbev/msab199.

Mao, Y. & Zhang, G. (2022) A complete, telomere-to-telomere human genome sequence presents new opportunities for evolutionary genomics. *Nature Methods*, 19, 635–638. https://doi.org/10.1038/s41592-022-01512-4.

Marchal, C., Michalopoulou, V.A., Zou, Z., Cevik, V. & Sarris, P.F. (2022) Show me your ID: NLR immune receptors with integrated domains in plants. *Essays in biochemistry*, 66, 527–539. https://doi.org/10.1042/EBC20210084.

Marelli, J.P., Guest, D.I., Bailey, B.A., Evans, H.C., Brown, J.K., Junaid, M., et al. (2019) Chocolate under threat from old and new cacao diseases. *Phytopathology*, 109, 1331–1343. https://doi.org/10.1094/PHYTO-12-18-0477-RVW.

Mistry, J., Chuguransky, S., Williams, L., Qureshi, M., Salazar, G.A., Sonnhammer, E.L.L., et al. (2021) Pfam: The protein families database in 2021. *Nucleic Acids Research*, 49, D412–D419. https://doi.org/10.1093/nar/gkaa913.

Motamayor, J.C., Lachenaud, P., Silva e Mota, J.W. da, Loor, R., Kuhn, D.N., Brown, J.S., et al. (2008) Geographic and genetic population differentiation of the Amazonian chocolate tree (Theobroma cacao L). *PLoS ONE*, 3. https://doi.org/10.1371/journal.pone.0003311.

Motamayor, J.C., Schnell, R., Kuhn, D., Phillips, W., Haiminen, N., Livingstone, D., et al. (2013) The genome sequence of the most widely cultivated cacao type and its use to identify candidate genes regulating pod color. *Genome Biology*, 14, r53.

Nousias, O., Zheng, J., Li, T., Meinhardt, L.W., Bailey, B., Gutierrez, O., et al. (2024) Three de novo assembled wild cacao genomes from the Upper Amazon. *Scientific data*, 11, 1–9. https://doi.org/10.1038/s41597-024-03215-1.

Orduña, H.E.N., Müller, M., Krutovsky, K. V & Gailing, O. (2024) Genotyping of cacao (Theobroma cacao L .) germplasm resources with SNP markers linked to agronomic traits reveals signs of selection. *Tree Genetics & Genomes*. https://doi.org/10.1007/s11295-024-01646-w.

Palmer, J.M. & Stajich, J.E. (2023) Funannotate. https://github.com/nextgenusfs/funannotate

Richardson, J.E., Whitlock, B.A., Meerow, A.W. & Madriñán, S. (2015) The age of chocolate: A diversification history of Theobroma and Malvaceae. *Frontiers in Ecology and Evolution*, 3, 1–14. https://doi.org/10.3389/fevo.2015.00120.

Santos, M. de L., Resende, M.L.V. de, Alves, G.S.C., Huguet-Tapia, J.C., Resende, M.F.R. de J. & Brawner, J.T. (2022) Genome-Wide Identification, Characterization, and Comparative Analysis of NLR Resistance Genes in Coffea spp. *Frontiers in Plant Science*, 13, 1–16. https://doi.org/10.3389/fpls.2022.868581.

Sayers, E.W., Cavanaugh, M., Clark, K., Pruitt, K.D., Sherry, S.T., Yankie, L., et al. (2023) GenBank 2023 update. *Nucleic Acids Research*, 51, D141–D144. https://doi.org/10.1093/nar/gkac1012.

Schnell, R.J., Kuhn, D.N., Brown, J.S., Olano, C.T., Amores, F.M. & Motamayor, J.C. (2007) Development of a Marker Assisted Selection Program for Cacao. Cacao Diseases : Important Threats to Chocolate Production Worldwide. Phytopathology.

Sergey, N., Sergey, K., Arang, R., Mikko, R., V., B.A., Alla, M., et al. (2022) The complete sequence of a human genome. *Science*, 376, 44–53. https://doi.org/10.1126/science.abj6987.

Sim, S.B., Corpuz, R.L., Simmonds, T.J. & Geib, S.M. (2022) HiFiAdapterFilt, a memory efficient read processing pipeline, prevents occurrence of adapter sequence in PacBio HiFi reads and their negative impacts on genome assembly. *BMC Genomics*, 23. https://doi.org/10.1186/s12864-022-08375-1.

Simão, F.A., Waterhouse, R.M., Ioannidis, P., Kriventseva, E. V. & Zdobnov, E.M. (2015) BUSCO: Assessing genome assembly and annotation completeness with single-copy orthologs. *Bioinformatics*, 31, 3210–3212. https://doi.org/10.1093/bioinformatics/btv351.

Singh, G. (2021) *Identification of Quantitative Trait Loci (QTL) associated with resistance to Vascular Streak Dieback disease of cacao*. The University of Sydney.

Sniezko, R.A. (2006) Resistance breeding against nonnative pathogens in forest trees — current successes in North America 1. *Canadian Journal of Plant Pathologu*, 279, 270–279.

Stanford, A.M., Harden, R. & Parks, C.R. (2000) Phylogeny and biogeography of Juglans (Juglandaceae) based on matK and ITS sequence data. *American Journal of Botany*, 87, 872–882. https://doi.org/10.2307/2656895.

Steuernagel, B., Witek, K., Krattinger, S.G., Ramirez-Gonzalez, R.H., Schoonbeek, H.J., Yu, G.,

et al. (2020) The NLR-annotator tool enables annotation of the intracellular immune receptor repertoire. *Plant Physiology*, 183, 468–482. https://doi.org/10.1104/pp.19.01273.

Sun, J., Lu, F., Luo, Y., Bie, L., Xu, L. & Wang, Y. (2023) OrthoVenn3: An integrated platform for exploring and visualizing orthologous data across genomes. *Nucleic Acids Research*, 51, W397–W403. https://doi.org/10.1093/nar/gkad313.

Thompson, J.D., Higgins, D.G. & Gibson, T.J. (1994) CLUSTAL W: improving the sensitivity of progressive multiple sequence alignment through sequence weighting, position-specific gap penalties and weight matrix choice. *Nucleic acids research*, 22, 4673–4680. https://doi.org/10.1093/nar/22.22.4673.

Tobias, P.A. (2024) Theobroma-cacao-genome. https://github.com/peritob/Theobroma-cacao-genome

Tobias, P.A., Edwards, R.J., Surana, P., Mangelson, H., Inácio, V., Céu Silva, M. do, et al. (2022) A chromosome-level genome resource for studying virulence mechanisms and evolution of the coffee rust pathogen Hemileia vastatrix *bioRxiv*, 2022.07.29.502101. https://doi.org/10.1101/2022.07.29.502101.

Tobias, P.A. & Guest, D.I. (2014) Tree immunity: growing old without antibodies. *Trends in plant science*, 19, 367–370. https://doi.org/10.1016/j.tplants.2014.01.011.

Trisno, J., Reflin, R. & Martinius, M. (2016) Vascular Streak Dieback: Penyakit Baru Tanaman Kakao di Sumatera Barat. *Jurnal Fitopatologi Indonesia*, 12, 142. https://doi.org/10.14692/jfi.12.4.142.

Weyer, A.-L. van de, Monteiro, F., Furzer, O.J., Nishimura, M.T., Cevik, V., Witek, K., et al. (2019) The Arabidopsis thaliana pan-NLRome. *bioRxiv*, 1–32. https://doi.org/10.1101/537001.

Weyer, A.L. Van de, Monteiro, F., Furzer, O.J., Nishimura, M.T., Cevik, V., Witek, K., et al. (2019) A Species-Wide Inventory of NLR Genes and Alleles in Arabidopsis thaliana. *Cell*, 178, 1260-1272.e14. https://doi.org/10.1016/j.cell.2019.07.038.

White, Bruns T, Lee S & Taylor, J. (1990) Amplification and direct sequencing of fungal ribosomal RNA genes for phylogenetics. PCR Protocols: A Guide to Methods and Application. San Diego, California: Academic Press, pp. 315–322.

Xi, Y., Cesari, S. & Kroj, T. (2022) Insight into the structure and molecular mode of action of plant paired NLR immune receptors. *Essays in biochemistry*, 66, 513–526.

Figure legends

Figure 1 Chromsyn (Edwards *et al.*, 2022) synteny plots of *Theobroma cacao* parentally phased genome, haplotype A (top) and B (below). Synteny blocks of collinear “Complete” BUSCO genes (Simão *et al.*, 2015) link scaffolds from adjacent assemblies: blue, same strand; red, inverse strand. Yellow triangles mark “Duplicated” BUSCOs. Filled circles mark telomere predictions from Telociraptor (black) (Edwards, 2023). Assembly gaps are marked as dark red + signs**.**

738 Figure 2 Physical locations of predicted NLR genes on the paired chromosomes of *Theobroma*
739 *cacao* (A) haplotype A (red) and (B) haplotype B (yellow) generated using ChromoMap (Anand
740 and Rodriguez Lopez, 2022) in RStudio.
741
742 Figure 3 The predicted NLR gene complement in the parentally phased *Theobroma cacao*
743 genome. The two sets of chromosomes corresponding to (above) Haplotypes A and (below)
744 B were independently classified (Chen *et al.*, 2023) and visualised to present the domain
745 classes using Sankeymatic (Bogart, 2014) including novel integrated domains (IDs) with
746 abbreviations derived from Pfam database (Mistry *et al.*, 2021). NB = Nucleotide Binding
747 Domain, TIR = Toll/Interleukin-1 receptor, Rx = Potato CC-NB-LRR protein Rx, CC=Coil-Coil
748 Domain, RPW8 = RESISTANCE TO POWDERY MILDEW 8-like coiled-coil**.**
749
750 Figure 4 Amino acid sequence alignment of an NLR cluster matching the QTL mapped regions
751 at around 29 Mb on chromosome three (above) and single NLR homologs at 31 Mb
752 chromosome nine (below) within both parentally inherited alleles, A and B, for *Theobroma*
753 *cacao* clone 26. All predicted NLRs are annotated as Rx-NLRs (Chen *et al.*, 2023) named for
754 resistance to potato virus X.
755
756 Figure 5 Leaf from *Theobroma cacao*, VSD susceptible clone 26, growing at the Mars Cocoa
757 Research Institute field trials, Pangkep South Sulawesi, Indonesia. (Left) The symptomatic leaf
758 apex dieback and some chlorosis indicating *Ceratobasium theobromae*. (Right) Visible
759 vascular death caused by the pathogen. Scale bar left ~5 cm**.**
760
761 Figure 6 *Theobroma cacao* resistant (S1) and susceptible (RUQ1347) parental paired-end (PE)
762 Illumina sequence reads mapped to the concatenated Hap A and B progeny chromosomes.
763 The reads that were mapped in greater numbers to chromosomes and contigs were used to
764 determine parental assignment and swapped accordingly.

765 ***Abbreviations***

766 NLR – nucleotide binding site leucine-rich repeat gene models
767 LRR – leucine-rich repeat domain
768 GB – gigabyte

Gb – Gigabase

Mb – Megabase

kb – kilobase

VSD – vascular streak dieback, causal agent *Ceratobasidium theobromae*

PPR – Phytophthora Pod Rot, causal agent *Phytophthora palmivora*